JPP JOURNAL OF Pharmacy and Pharmacology
ROYAL PHARMACEUTICAL SOCIETY
JPP Journal of Pharmacy And Pharmacology
Research Paper

# Non-inclusion complexes between riboflavin and cyclodextrins

Marcelo Bispo de Jesus[a], Leonardo Fernandes Fraceto[a,b], Maria Florencia Martini[c], Monica Pickholz[a,c], Carmen Veríssima Ferreira[a] and Eneida de Paula[a]

[a]Department of Biochemistry, Institute of Biology, State University of Campinas (Unicamp), Campinas, [b]Department of Environmental Engineering, State University of São Paulo (Unesp), Sorocaba, Brazil and [c]Department of Pharmaceutical Technology, Faculty of Pharmacy and Biochemistry, University of Buenos Aires and CONICET, Argentina

**Keywords**
cyclodextrin; NMR; non-inclusion complex; prostate cancer; riboflavin

**Correspondence**
Eneida de Paula, Department of Biochemistry, Institute of Biology, State University of Campinas, PO Box 6109, CEP 13083-970, Rua Monteiro Lobato, 255 – Campinas, SP, Brazil.
E-mail: depaula@unicamp.br

Received August 24, 2011
Accepted January 27, 2012

doi: 10.1111/j.2042-7158.2012.01492.x

## Abstract

**Objectives** To investigate the molecular interaction between β-cyclodextrin (βCD) or hydroxypropyl-β-cyclodextrin (HPβCD) and riboflavin (RF), and to test the anticancer potential of these formulations.

**Methods** The physicochemical characterization of the association between RF and CDs was performed by UV-vis absorption, fluorescence, differential scanning calorimetry and NMR techniques. Molecular dynamics simulation was used to shed light on the mechanism of interaction of RF and CDs. Additionally, in-vitro cell culture tests were performed to evaluate the cytotoxicity of the RF–CD complexes against prostate cancer cells.

**Key findings** Neither βCD nor HPβCD led to substantial changes in the physicochemical properties of RF (with the exception of solubility). Additionally, rotating frame Overhauser effect spectroscopy experiments detected no spatial correlations between hydrogens from the internal cavity of CDs and RF, while molecular dynamics simulations revealed 'out-of-ring' RF–CD interactions. Notwithstanding, both RF–βCD and RF–HPβCD complexes were cytotoxic to PC3 prostate cancer cells.

**Conclusions** The interaction between RF and either βCD or HPβCD, at low concentrations, seems to be made through hydrogen bonding between the flavonoid and the external rim of both CDs. Regardless of the mechanism of complexation, our findings indicate that RF–CD complexes significantly increase RF solubility and potentiate its antitumour effect.

## Introduction

Prostate cancer is a significant public health problem and can be fatal in men.[1] Declines in prostate cancer mortality are expected with improvements in early-stage detection.[2] However, the clinical management of prostate cancer, with its aggressive and highly metastatic phenotypes, continues to be challenging and novel adjuvant strategies are urgently required.[3]

Riboflavin (RF) is part of the vitamin B complex and is a potent photosensitizer. RF photodegradation includes intramolecular photoreduction and photoaddition, and its major photoproducts are 7,8-dimethyl-10-(formylmethyl) isoalloxazine (formylmethylflavin), lumichrome, 2′-ketoriboflavin 4′-ketoriboflavin and lumiflavin. We have shown that the photoproducts of RF diminish survival signalling in both leukaemia and prostate cancer cells. Importantly, the toxic effect was strictly dependent on the presence of riboflavin photoproducts, since non-irradiated riboflavin had no influence on tumour cell growth.[4,5] In addition, RF and pyridoxal 5′-phosphate may inhibit colorectal tumourigenesis in humans.[6] Thus, RF has great pharmacological potential, taking into consideration its physiological role, relative low cost and anticancer activity. However, the relatively poor water solubility and photosensitivity of RF limit its application.[7,8] We therefore decided to combine RF with cyclodextrins (CDs), as these cyclic oligosaccharides have been used extensively as successful drug delivery carriers. The interaction of amphiphile compounds with CDs may increase their water solubility, diminish their effective doses,

decrease their toxic side-effects, and protect the compounds against dehydration, hydrolysis, oxidation and photodegradation. Such effects have improved the pharmaceutical properties of several drugs.[9]

Although inclusion complexes are the most common and best described interaction between CDs and guest molecules, a number of non-inclusion complexes have also been described,[10–13] in which self-assembled nanoaggregates (but not inclusion complexes) lead to solubilization of poorly soluble compounds (for a review see Messner *et al*.[12]).

In this study, we have used different physicochemical approaches to characterize the complexes formed between RF and β-cyclodextrin (βCD) or hydroxypropyl-β-cyclodextrin (HPβCD) at different molar ratios. Complexation increased RF solubility and, most importantly, its antiproliferative activity towards prostate cancer cells.

## Materials and Methods

Riboflavin, βCD, benzocaine and RPMI 1640 cell culture medium were obtained from Sigma Chemical Co. (Taufkirchen, Germany). HPβCD (Kleptose HP) was purchased from Roquette Serv. Tech. Lab. (Lestrem, Cedex, France). All other chemicals used were of analytical grade.

### Preparation of RF–βCD and RF–HPβCD complexes

We have combined RF (300 μM) and equivalent molar fractions of CDs (βCD or HPβCD) in water for 3 h to ensure equilibrium. The samples were freeze-dried and stored at –20°C for further use.

Pure RF samples were also submitted to the freeze-drying process, to be used as a control in biological tests. All technical procedures were conducted in darkness to avoid RF photodegradation.

### Kinetics of RF–CD complexation

The kinetics of association were determined by following the RF absorption at 444 nm after addition of different molar ratios of βCD (up to 1 : 15) or HPβCD (up to 1 : 120) under agitation as a function of time (8 h). The experiments were done at 25°C, in duplicate.

### Phase solubility isotherms

Solubility studies were performed according to the methodology described by Higuchi and Connors.[14] Briefly, an excess amount of solid RF (to give a final 1 mM concentration) was added to different βCD (0, 1, 2, 4, 8, 12 and 16 mM) or HPβCD (0, 10, 20, 40, 80, 120 and 160 mM) solutions. Samples were kept under agitation until equilibrium (for 3 h as determined in the kinetics experiments). Samples were filtered through 0.22-μm membranes and RF quantification was spectrophotometrically performed at 444 nm, accordingly to a previously determined analytic curve (absorbance = 0.012 × concentration (M), $r = 0.999$). The experiments were carried out in triplicate.

### Fluorescence experiments

Emission spectra were recorded in a F-4500 fluorimeter (Hitachi, Tokyo, Japan). Samples of RF in the presence or absence of CDs were excited at 374 nm and the emission was followed from 450 nm to 650 nm. The experiments were carried out in triplicate at 25°C.

### Differential scanning calorimetry

Differential scanning calorimetry was performed using a Universal V2.3D TA instrument (New Castle, DE, USA). Samples of 5–10 mg were placed at aluminium crimped cells and submitted to a graduated increase in temperature (10°C/min) from 30°C to 260°C under an inert atmosphere. The following lyophilized samples were analysed: pure compounds (RF, βCD, HPβCD), non-inclusion complexes (RF–βCD and RF–HPβCD) and their physical mixture (RF–βCD and RF–HPβCD) in equivalent molar fractions. The experiments were carried out in duplicate.

### Nuclear magnetic resonance

One- and two-dimensional $^1$H-NMR spectra were recorded on Varian Inova 500 MHz (11.75 T) equipment at the Brazilian Synchrotron Light Laboratory (LNLS, Campinas, SP, Brazil). Samples of an equivalent concentration (150 μM) of RF and βCD or HPβCD were prepared in $D_2O$, homogenized for 3 h and transferred to 5-mm tubes for spectrum acquisition. The residual water peak (4.87 ppm) was used as a reference. No external references were used to avoid possible interactions with CDs.[15] and at least two different experiments were conducted at 20°C with different samples in different days.

Diffusion ordered spectroscopy experiments were carried out using the BPPSTE (bipolar pulse pairs stimulated echo) sequence.[16] The duration of the total diffusion-phase encoding the gradient pulse was 2 ms, the diffusion delay was 0.05 s, and the minimum gradient strength was set to 0.3 G/cm. The diffusion coefficients were measured for the pure compounds (RF, βCD, HPβCD) and for the RF–CD complexes (1 : 1 molar ratio).

Longitudinal relaxation times ($T_1$) were obtained by the conventional inversion-recovery technique[17] in RF and 1 : 1 RF–βCD samples. Typical acquisition parameters consisted of 10–15-μs 90° pulses, 16 scans and 16 recovering time intervals in a 12-ppm window; the recycling time was set to 5 times the largest $T_1$ (those of the aromatic hydrogens of RF).

Rotating frame Overhauser effect spectroscopy experiments were carried out using the standard pulse sequence of the equipment.[17] The acquisition parameters used were a magnetic field strength of 11.75 T, a mixing time of 300 ms, spectral window of 10 ppm, 2048 k in F2 and 324 increments. Data processing was conducted using NMRView and NMRpipe software (One Moon Scientific, Westfield, NJ, USA).

### Molecular dynamics simulation setup

The interaction between RF and βCD was investigated using molecular dynamic simulations performed by the GROMACS 4.0 software package (Uppsala, Sweden).[18–21] The GROMOS-96 53a6 force field[22] was used for both RF and βCD molecules. The electrostatic interactions were handled with the SPME version of the Ewald sum.[23,24]

The settings for the SPME method were a real space cut-off of 1.4 nm, a grid spacing of 0.12 nm and a cubic interpolation. In all the simulations, the van der Waals interactions were cut off at 1.4 nm. The simulations were carried out in the NVT ensemble using the Berendsen thermostat.[25] The whole system was coupled to a temperature bath with a reference temperature of 300 K and a relaxation constant of 0.1 ps. No constraints were used for the bonds. The time step for the integration of the equation of motion was 1 fs. The non-bonded list was updated every 10 steps. To release steric clashes, we performed 1 000 000 steepest descent cycles and 1 000 000 steps of the conjugated gradient algorithm. Prior to the production run, a series of four equilibration steps of 100 ps each was performed, upgrading the temperature progressively.

The simulated system consisted in eight pairs of RF and βCD. Each pair was built in a cubic box, using the Packmol package (Campinas, Brazil)[26] sampling different orientations of the RF molecule with respect to the βCD and 12 000 SPC water molecules.[27] These boxes were assembled as the eight quadrants of the simulation cubic box and molecular dynamics simulations were carried out up to the 50-ns production run. The images ware made with VMD software. VMD was developed with NIH support by the Theoretical and Computational Biophysics group at the Beckman Institute, University of Illinois at Urbana-Champaign, USA.

### Cell culture

The PC3 cell line was purchased from the American Type Culture Collection (Rockville, MD, USA) and grown according to their guidelines. Cells were cultured in RPMI 1640 media containing 10% fetal bovine serum, 100 U/ml penicillin and 100 μg/ml streptomycin, in a humidified incubator at 37°C with 5% $CO_2$.

Cells ($10^4$ per well) were incubated in 96-well plates until semiconfluence. They were then treated for 24 h with the pure compounds (RF, βCD, HPβCD) or with the complexes (RF–βCD or RF–HPβCD, in a 1 : 1 molar ratio). Experiments were conducted in triplicate for each treatment and cell viability was assessed by the 3-(4,5-dimethylthiazol-2-yl)-2,5-diphenyl tetrazolium bromide (MTT) reduction assay.

### MTT reduction assay

After 24 h of treatment, the medium was replaced with a MTT solution (100 μl, 0.5 mg/ml of media) and incubated for 4 h at 37°C. The medium was then removed and DMSO (100 μl) was added to dissolve the formazan crystals. The plates were agitated for 5 min and the formazan absorbance was measured at 570 nm using a microplate reader (Model 7530; Cambridge Technology Inc., Lexington, MA, USA). Cell viability was plotted as a percentage of the control.[28]

### Statistical analysis

Cytotoxic assay data were analysed by one-way analysis of variance with the Tukey-Kramer post-hoc test. Statistical significance was defined as $P < 0.05$.

## Results and Discussion

### Physicochemical characterization of the RF–CD interaction

Initially, the kinetics of association was followed for 8 h through changes in RF absorbance at 444 nm. Changes in RF absorbance were not registered after the first hour, suggesting a fast interaction between RF and both CDs (data not shown).

Phase solubility[14] studies revealed that RF solubility (Figure 1) was increased 1.6 times by 16 mM βCD and 4.2 times by 150 mM HPβCD. The limited water solubility of βCD did not allow the experiments to be conducted at

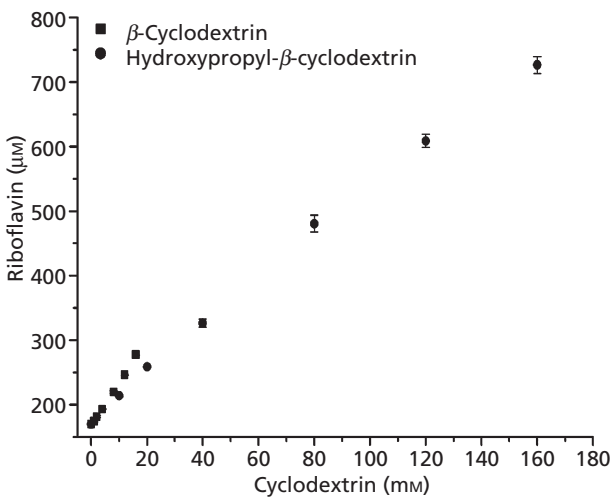


**Figure 1** Phase solubility diagrams of riboflavin in β-cyclodextrin and hydroxypropyl-β-cyclodextrin at 25°C ($n = 3$).

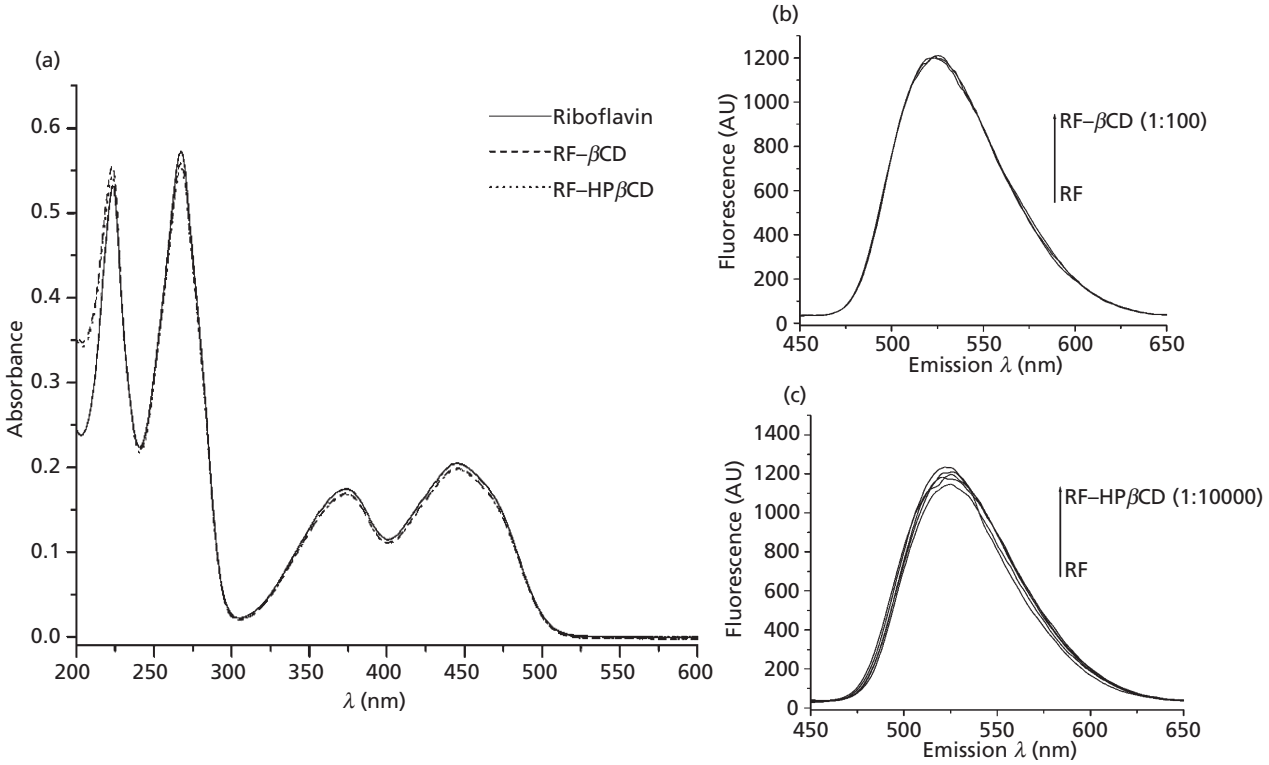


**Figure 2** (a) UV-vis absorption spectra of riboflavin (RF) in the presence of equivalent *β*-cyclodextrin (*β*CD) or hydroxypropyl-*β*-cyclodextrin (HP*β*CD) concentrations. (b),(c) Fluorescence emission spectra of RF in the absence and presence of increasing *β*CD (up to 1 : 100 mole%) or HP*β*CD (1 : 10 000 mole%). Riboflavin concentration = 10 μM, $n = 3$.

concentrations higher than 16 mM.[29] The linear increase in RF solubility in the presence of CDs (Figure 1) suggested a first-order complex and a 1 : 1 stoichiometry of complexation. Assuming that, the association constants were calculated[14] for RF either with *β*CD (39.7/M ± 0.31) or HP*β*CD (20.6/M ± 0.22). These values denote a very weak interaction between RF and CDs, and they are in good agreement with previously reported values.[30,31] It is worth noting that solubility isotherms do not establish conclusively if real complexation takes place once CDs are able to form non-inclusion complexes which can solubilize guest molecules in aggregate structures.[12,32]

We investigated the interaction of RF with both CDs through changes in the UV-vis absorption spectrum (Figure 2a), which could provide information about the transfer of guest molecules from water to the hydrophobic cavity of CD.[33] A slight decrease in RF absorption was observed for the peaks at 266, 374 and 444 nm, in agreement with the previous observation by Wang and Chen.[34] Those authors also found that the RF absorption properties in the presence of CDs were comparable with those of RF in ethanol solution, based on a hypsochromic shift in the 374-nm peak. Our results, however, did not show such change in the RF absorption spectrum, either in the presence of *β*CD or HP*β*CD (Figure 2a).

Differential scanning calorimetry has been used to characterize the solid-state of inclusion complexes formed by CDs (data not shown). The characteristic endothermic broad peak of pure *β*CD was observed near 160°C, which is assigned to the loss of water from the *β*CD cavity[35,36] during the heating process. The RF–*β*CD physical mixture thermogram still presented this residual water peak, which was expected if no inclusion complex was formed. Surprisingly, a residual peak was also observed near 160°C for the RF–*β*CD complex sample, suggesting that even after co-solubilization of RF and CD, the water molecules inside the CD were not replaced by the guest (RF) molecule.[36] Similar results were observed for HP*β*CD; thermograms of pure HP*β*CD, its physical mixture with RF and the RF–HP*β*CD complex were indistinguishable and there was no evidence of inclusion complexation. This lack of evidence is compatible with a weak RF–CD interaction (low association constants) and also with CDs 'out-of-ring' complexation.

We also investigated the fluorescence of RF in the presence of *β*CD (Figure 2b) and HP*β*CD (Figure 2c). CDs cavities could affect the intrinsic fluorescence of guest compounds

**Table 1** $^1$H-NMR chemical shift of riboflavin hydrogens, $\beta$-cyclodextrin and hydroxypropyl-$\beta$-cyclodextrin in $D_2O$, at 20°C, 500 MHz

| RF (0.15 mM) | | | | | | $\beta$CD (0.15 mM) | | | | HP$\beta$CD (0.15 mM) | | | |
|---|---|---|---|---|---|---|---|---|---|---|---|---|---|
| 1H | In $D_2O$ | With $\beta$CD | Δ (ppm) | With HP$\beta$CD | Δ (ppm) | 1H | In $D_2O$ | With RF | Δ (ppm) | 1H | In $D_2O$ | With RF | Δ (ppm) |
| 7-CH3 | 2.41 | 2.43 | –0.02 | 2.43 | –0.02 | H4 | 3.56 | 3.55 | 0.01 | H4 | 3.46 | 3.45 | 0.01 |
| 8-CH3 | 2.52 | 2.53 | –0.01 | 2.53 | –0.01 | H2 | 3.62 | 3.61 | 0.01 | H2 | 3.57 | 3.56 | 0.01 |
| 5b′ | 3.69 | nd | nd | nd | nd | H5 | 3.84 | 3.84 | 0.00 | H5 | 3.81 | 3.81 | 0.00 |
| 5a′ | 3.84 | nd | nd | nd | nd | H6 | 3.85 | 3.85 | 0.00 | H6 | 3.84 | 3.84 | 0.00 |
| 4′ | 3.89 | nd | nd | nd | nd | H3 | 3.94 | 3.93 | 0.01 | H3 | 3.92 | 3.92 | 0.00 |
| 3′ | 3.94 | nd | nd | nd | nd | H1 | 5.05 | 5.04 | 0.01 | H1 | 5.04 | 5.02 | 0.02 |
| 2′ | 4.40 | 4.39 | 0.01 | 4.39 | 0.01 | | | | | -CH3 | 1.11 | 1.10 | 0.01 |
| 1′ | 5.09 | 5.06 | 0.03 | nd | nd | | | | | | | | |
| 6 | 7.93 | 7.92 | 0.01 | 7.90 | 0.03 | | | | | | | | |
| 9 | 7.94 | 7.92 | 0.02 | 7.91 | 0.03 | | | | | | | | |
| N-H | 8.11 | nd | nd | nd | nd | | | | | | | | |

Assignments of RF and CDs according to Grillo et al. and Pinto et al.[41,45]. RF, riboflavin; RF–$\beta$CD, riboflavin–$\beta$-cyclodextrin complex; RF–HP$\beta$CD, riboflavin–hydroxypropyl-$\beta$-cyclodextrin complex; nd, not determined due to peak overlapping in this region of the spectra.

that are sensitive to solvent polarity or dielectric properties.[37] Nevertheless, even at a high molar ratio of RF to HP$\beta$CD (1 : 10 000), only a slight change was observed in RF fluorescence. Again, no evidence of inclusion complex formation was obtained. It is worth noting that RF fluorescence does show significant hyper and hypsochromic shifts when exposed to hydrophobic environments such as methanol.

The absence of changes in the differential scanning calorimetry thermograms, UV-vis (Figure 2a) or fluorescence (Figure 2b and 2c) spectra of RF in the presence of CDs led us to consider that RF did not form an inclusion complex with any CD tested. This hypothesis required us to conduct a deeper investigation into the RF–CD interaction using NMR and molecular dynamics approaches.

## The non-inclusion hypothesis

Different NMR approaches were used to achieve details on the molecular interaction between RF and CDs.[38–41] The $^1$H-NMR assignment of RF peaks (see Table 1 and the inset of Figure 3) are in good agreement with the literature.[42–44]

In the presence of $\beta$CD and HP$\beta$CD, no significant changes in the chemical shifts of RF or $\beta$CD hydrogens were detected (Table 1), in accordance with the reported UV-vis and fluorescence results. The lack of changes in $^1$H-NMR chemical shifts (Table 1) of $H_3$ and $H_5$ peaks of CDs provides strong evidence that RF does not form any inclusion complex with the CDs. These hydrogens are known to monitor the CD cavity interior.[41,45,46] Accordingly, Zielenkiewicz *et al*.[31] found no changes in the HP$\beta$CD spectra in the presence of RF, and attributed this to the low RF solubility. These authors have also reported slight changes (0.05–0.08 ppm) in $^1$H-NMR chemical shifts of the $H_6$ and $H_9$ aromatic hydrogens of RF in the presence of a high HP$\beta$CD concentration.[31] However, our NOE (Figure 4) and molecular dynamics (Figure 6) results indicate that these changes can be assigned to $\pi$–$\pi$ stacking of RF.

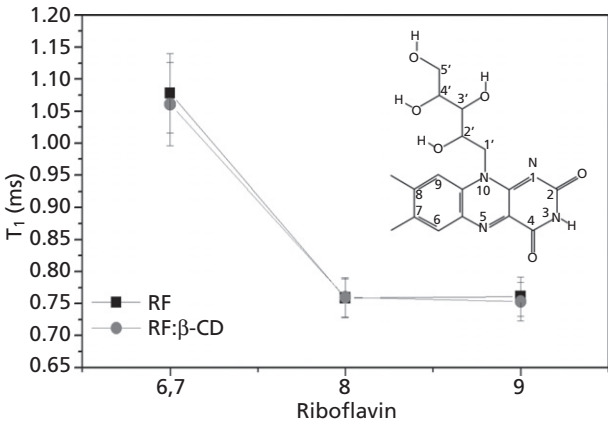


**Figure 3** Longitudinal relaxation times ($T_1$, ms) of the aromatic riboflavin (RF) hydrogens in $D_2O$ and in the presence of $\beta$-cyclodextrin (RF–$\beta$CD).

Longitudinal relaxation times ($T_1$) are known to be strongly affected by the local environment of the $^1$H nucleus, decreasing as it interacts with the molecular net around it.[47] In this way, $T_1$ values measured from the $^1$H-NMR spectrum of guest compounds are expected to decrease upon complexation with CDs.[41,48] The $T_1$ values of the RF aromatic hydrogens 6–9, measured in the presence and absence of $\beta$CD are presented in Figure 3; unfortunately, superposition of peaks did not allow precise measurement of the $T_1$ value for the ribityl RF hydrogens. No changes were detected in the $T_1$ values of hydrogens belonging to the methyl groups of the aromatic carbons 7 and 8 (Figure 3) or adjacent aromatic hydrogens, at carbons 6 and 9 of RF. Similar results were observed for HP$\beta$CD (not shown). Overall, the $T_1$ results indicated that RF hydrogens were in fast exchange (in the NMR timescale), since no changes in the dynamic properties of the molecule were observed in the presence of CDs that could be assigned to the formation of an inclusion complex.

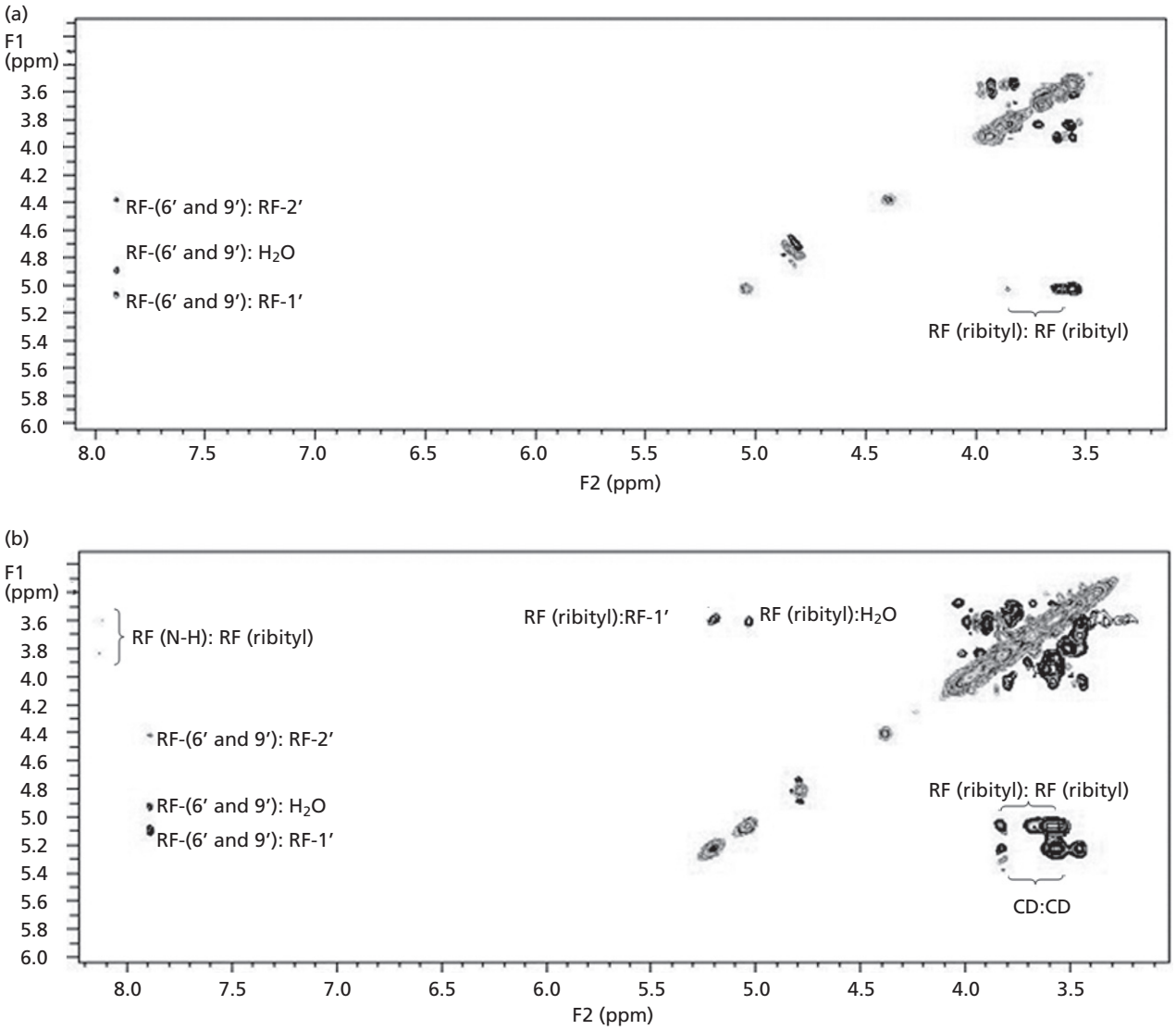


**Figure 4** Expansion of the bidimensional $^1$H-NMR ROESY spectra of riboflavin–$\beta$-cyclodextrin complex (1 : 1 molar ratio, 150 μM; a) and riboflavin–hydroxypropyl-$\beta$-cyclodextrin complex (1 : 1 molar ratio, 150 μM; b) at 500 MHz, 20°C, mixing time = 250 ms.

Diffusion ordered spectroscopy is another useful NMR technique to detect CD guest–host complex formation.[39,49] The diffusion coefficient determined through diffusion ordered spectroscopy experiments for pure RF ($3.23 \pm 0.16 \times 10^{-10}$ m$^2$/s) showed only minor changes when RF interacted with $\beta$CD ($3.13 \pm 0.14 \times 10^{-10}$ m$^2$/s) or HP$\beta$CD ($3.15 \pm 0.14 \times 10^{-10}$ m$^2$/s). This result suggests weak RF–CD interactions, as in the case of non-inclusion intermolecular complexation. Moreover, the small changes in diffusion coefficient did not allow the determination of the RF fraction bound to the CDs or the association constant, in clear opposition with the results obtained when guest–host inclusion complexes are formed.[38,39]

As a final NMR approach, we used nuclear Overhauser (rotating frame Overhauser effect spectroscopy; NOE) experiments to check the dipolar–dipolar (through the space) interactions[38,45] between RF and CDs (Figure 4). Intramolecular NOEs were just detected between the aromatic ($H_6$, $H_9$) and $H_{2'}$ or between ($H_6$, $H_9$) and $H_{1'}$ ribityl hydrogens of RF and in between ribityl hydrogens of RF (Figure 4), revealing the dynamics of the riboflavin molecule in the presence of both CDs. Peak superposition at 4.05 ppm (Table 1) did not allow us to conclude if the other NOE peaks observed in Figure 4 involving $H_6$ and $H_9$ aromatic hydrogens of RF were due to inter (RF–CD) or intra (RF–RF) molecular interaction. The RF : RF NOE peaks observed between $H_6$/$H_9$

and $H_1$ or $H_{2'}$ of RF are consistent with stacking or riboflavin $\pi$-dimer formation, as discussed below. Notably, no intermolecular correlation peaks were observed between RF and hydrogens from the CD internal cavity ($H_3$ and $H_5$, the hydrogens usually implied in the case of molecule inclusion inside the cavity) of $\beta$CD or HP$\beta$CD to sustain the RF–CD inclusion complex formation.

The lack of NOE effect on the hydrogens in the inner cavity of CDs strongly suggests the formation of non-inclusion complexes. To shed light on the intermolecular interactions between RF and CDs we carried out extensive molecular dynamics simulations.

## RF–CD complex topology

The initial condition for molecular simulations comprised eight pairs of RF and $\beta$CD. Each pair was set in one of the quadrants of the simulation box, having different (and representative) RF/$\beta$CD relative orientations. These orientations were chosen to provide a good sampling of the possible complexes formation.

In Figure 5 we show four snapshots of the eight RF–$\beta$CD pairs at four different times of simulation. The four snapshots correspond to the initial time (a), 5 ns (b), 25 ns (c) and 45 ns (d) of simulation. After 5 ns, we could see the nucleation of a cluster involving both $\beta$CD and RF molecules (see additional supporting information: Movies S1 and S2). With time, the cluster grew up to a regimen where all the RF molecules and six of the eight $\beta$CDs were involved. The tendency of CD to form clusters is well known, the cluster tending to increase with higher CD concentration and with the formation of guest–host inclusion complexes (for a review see Messner *et al*.[12]). In our case, most RF was not found inside the $\beta$CD cavity. In fact, just one RF molecule (initially placed inside the $\beta$CD) remained there, probably due to entropic reasons. Furthermore, by means of radial pair distribution function and angle analysis, we have found that RF can stack, forming $\pi$-dimers. These could explain the NOE peaks observed between $H_6/H_9$ and $H_{1'}$ of RF (Figure 4).

Overall, the experimental (differential scanning calorimetry and spectroscopic) results strongly suggest that in the presence of CDs the increase in RF water solubility is a result

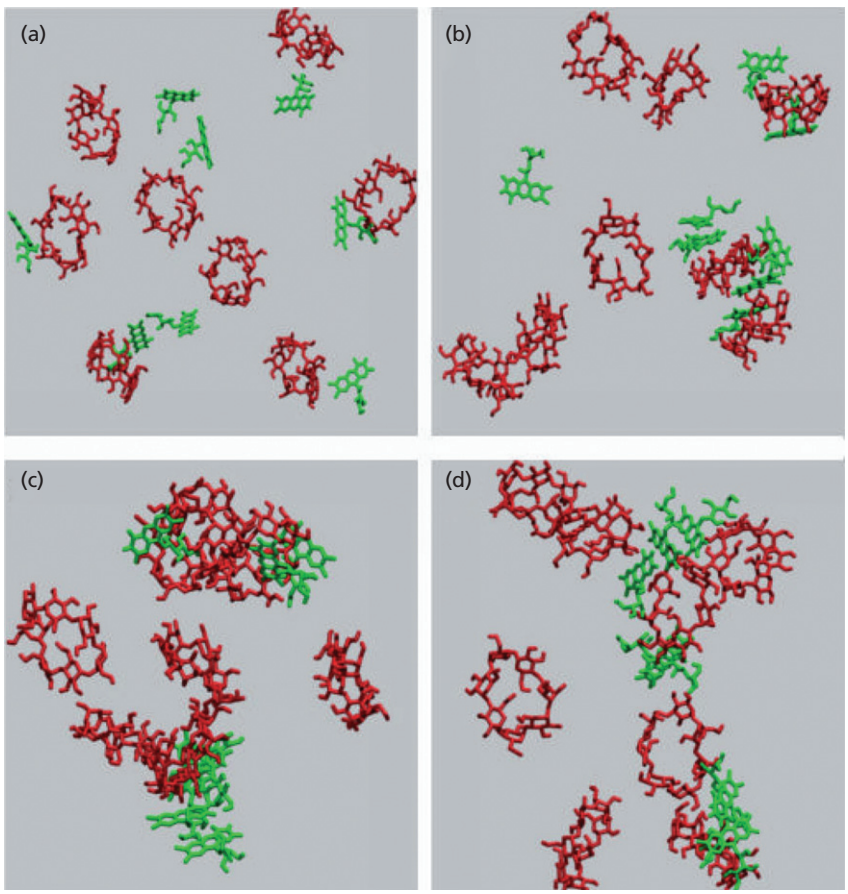


**Figure 5** Snapshots of the eight riboflavin-$\beta$-cyclodextrin pairs at different times in the molecular dynamics simulation run. (a) t = 0 ns. (b) t = 5 ns. (c) t = 25 ns. (d) t = 45 ns.

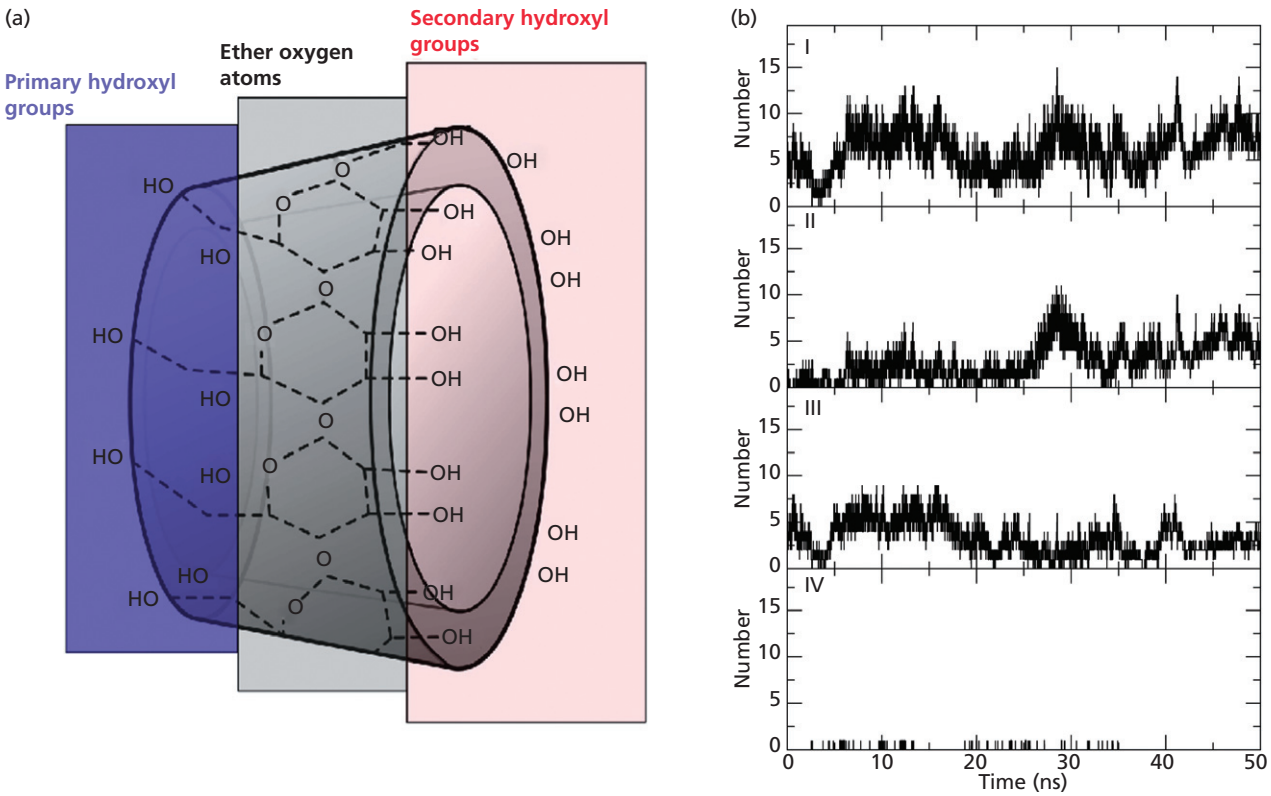


**Figure 6** (a) Types of oxygen atoms of the β-cyclodextrin structure. (b) Number of hydrogen bonds formed between riboflavin and the different types of oxygen groups of β-cyclodextrin as function of the simulation time: I, all oxygen groups; II, the secondary hydroxyl groups; III, the primary hydroxyl groups; and IV, the ether oxygen atoms (glycosidic oxygen bridges).

of non-inclusion complex formation. We studied the host–guest interactions between RF and βCD to describe the topology of the non-inclusion complex based on our simulation results. To that end, we divided the oxygen atoms of βCD into three types (Figure 6a): (1) the secondary hydroxyl groups, situated at the wider edge of the molecule; (2) the primary hydroxyl groups, situated at the narrow edge of the molecule; and (3) the glycosidic oxygen bridges, which are directed toward the inside of the cavity, which produce a high electron density, giving it some Lewis base characteristics.[29] Additionally, it has been reported that the ribityl substituent prevents deeper insertion of RF into the CD cavity.[31] We calculated the number of hydrogen bonds formed during the simulation run, between the eight RF molecules and the three different types of oxygen atoms of the eight βCD molecules. In Figure 6b we show the number of hydrogen bonds as a function of the time for all oxygen groups (I), the secondary hydroxyl groups (II), the primary hydroxyl groups (III) and the ether oxygen atoms (IV). Hydrogen bond interactions were essentially observed between RF and primary and secondary hydroxyl groups. We have estimated the number of hydrogen bond formations per step, per molecule of βCD. This number was around ~0.35 for both primary and secondary hydroxyl βCD groups with RFs. However, no significant hydrogen bond values (<0.01) were found between RF and the ether oxygen atoms.

These results support the experimental data and show that RF did not reach the βCD hydrophobic cavity, under the tested conditions. Furthermore, the formation of non-inclusion complexes can be inferred from the experimental and theoretical analysis. Finally, regardless of the type interaction detected between RF and CDs, we examined the effect of RF and RF–CD complexes on prostate cancer (PC3) cells.

## RF–CD complexes improve RF antitumour activity

PC3 is a fast growing cell type remarkably resistant to chemotherapeutic intervention. We tested the effect of RF alone and combined with βCD or HPβCD on the survival of these cancer cells (Figure 7). Neither βCD nor HPβCD in equivalent concentrations (0–100 μM) presented any toxic effects on PC3 cells.

The greatest effect of RF on prostate cancer cells was observed at 100 μM (Figure 7). Interestingly, PC3 cells were more sensitive to RF when the vitamin formed non-inclusion



 

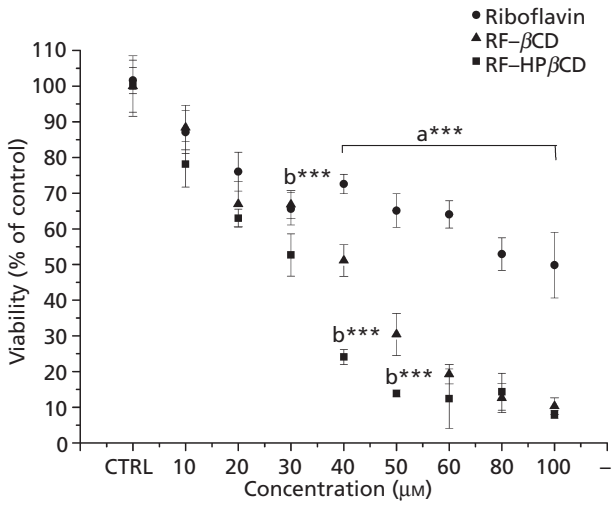


**Figure 7** Cytotoxic effects of riboflavin (RF), riboflavin–$\beta$-cyclodextrin complex (RF–$\beta$CD) and riboflavin–hydroxypropyl-$\beta$-cyclodextrin complex (RF–HP$\beta$CD) on PC3 prostate cells. PC3 cells were treated with RF, RF–$\beta$CD or RF–HP$\beta$CD for 24 h and the cell viability was measured by the MTT assay; the cell viability of non-treated cells was considered as 100% (mean ± SD, $n = 3$ experiments). Statistical differences are shown between: (a) RF–$\beta$CD or RF–HP$\beta$CD *vs* RF; (b) RF–HP$\beta$CD *vs* RF–$\beta$CD ***$P < 0.001$ (one-way analysis of variance with the Tukey-Kramer post-hoc test).

complexes with $\beta$CD or RF–HP$\beta$CD ($P < 0.001$% at concentrations of 40–100 μM). The improved cytotoxic profile observed for the RF–CD complexes could be explained by the increased solubility of riboflavin, justifying also the slightly better performance of RF–HP$\beta$CD over RF–$\beta$CD at concentrations of 30–50 μM ($P < 0.001$%; Figure 7). As for the classic inclusion complexation, RF and CD interactions are weak and do not curb the vitamin association with the cell membrane. Therefore, the interaction with CDs might favour RF uptake by prostate cancer cells via endocytosis. Bareford *et al*.[50] published an elegant study about RF absorption by breast cancer cells showing that the concentration of RF can be crucial to determine the mechanism of transport, as well as to maintain the cellular homeostasis of this micronutrient as a dynamic and controlled process.

## Conclusions

Molecular level knowledge of the interaction between drugs and CDs is crucial in the development of new formulations.[51] Here we characterized the interaction between RF and CDs, where the contribution of inclusion complexation was negligible. We based this conclusion on the low association constants and the absence or almost undetectable changes in the physicochemical properties of RF (with the exception of solubility) in the presence of CDs.

The interaction between RF and $\beta$CD or HP$\beta$CD and CDs, at low concentrations, seems to be mostly through non-inclusion complex formation. In fact, rotating frame Overhauser effect spectroscopy experiments detected no spatial correlations between hydrogens of RF and $H_3$ and $H_5$ hydrogens (from the internal cavity of $\beta$CD and HP$\beta$CD), and molecular dynamics simulations confirmed this 'out-of-ring' RF interaction.

The solubility of RF increased as an result of its association with both CDs, and the cytotoxicity of RF against PC3 prostate cancer cells also increased. This work describes in detail the formation of complexes between RF and $\beta$CD or HP$\beta$CD that are not based on the inclusion of RF into the CD cavity but still present a significant effect on the biological role of riboflavin. Non-inclusion complexation is an alternative mechanism of guest–CD interaction that could lead to physicochemical and pharmaceutical improvement of compound properties.

## Declarations

### Conflict of interest

The Authors declare that they have no conflicts of interest to disclose.

### Funding

São Paulo Research Foundation (FAPESP) supported this research. MBJ, EP and MP were the recipients of fellowships from FAPESP (Proc no. 06/03838-1), the National Council for Scientific and Technological Development (CNPq, Brazil) and the National Science Research Council (CONICET, Argentina), respectively.

### Acknowledgements

The authors also would like to thank the Brazilian Synchrotron Light Laboratory for use of the NMR facilities.

## References

1. Jemal A *et al*. Cancer statistics, 2010. *CA Cancer J Clin* 2010; 5: 277–300.
2. Malvezzi M *et al*. European cancer mortality predictions for the year 2011. *Ann Oncol* 2011; 4: 947–956.
3. Zelefsky MJ *et al*. Metastasis after radical prostatectomy or external beam radiotherapy for patients with clinically localized prostate cancer: a comparison of clinical cohorts adjusted for case mix. *J Clin Oncol* 2010; 9: 1508–1513.
4. Souza ACS *et al*. A promising action of riboflavin as a mediator of leukaemia cell death. *Apoptosis* 2006; 10: 1761–1771.
5. de Souza Queiroz KC *et al*. A possible anti-proliferative and anti-metastatic effect of irradiated riboflavin in solid

tumours. *Cancer Lett* 2007; 1: 126–134.
6. Figueiredo JC *et al*. Vitamins B2, B6, and B12 and risk of new colorectal adenomas in a randomized trial of aspirin use and folic acid supplementation. *Cancer Epidemiol Biomarkers Prev* 2008; 8: 2136–2145.
7. Aniceto C *et al*. Determinação Espectrofotométrica de Vitamina B2 (Riboflavina) em Formulações Farmacêuticas Empregando Sistema de Análises por Injeção em Fluxo. *Quim Nova* 2000; 5: 637–640.
8. Ball GFM. *Vitamins. Their Role in the Human Body*. London: Blackwell Publishing, 2004.
9. Laza-Knoerr AL *et al*. Cyclodextrins for drug delivery. *J Drug Target* 2010; 9: 645–656.
10. Mohamed MH *et al*. Electrospray ionization mass spectrometry studies of cyclodextrin-carboxylate ion inclusion complexes. *Rapid Commun Mass Spectrom* 2009; 23: 3703–3712.
11. Ribeiro RR *et al*. Prolonged absorption of antimony(V) by the oral route from non-inclusion meglumine antimoniate-beta-cyclodextrin conjugates. *Biopharm Drug Dispos* 2010; 2–3: 109–119.
12. Messner M *et al*. Self-assembled cyclodextrin aggregates and nanoparticles. *Int J Pharm* 2010; 1–2: 199–208.
13. Jansook P *et al*. yCD/HPyCD mixtures as solubilizer: solid-state characterization and sample dexamethasone eye drop suspension. *J Pharm Pharm Sci* 2010; 3: 336–350.
14. Higuchi T, Connors KA. Phase-solubility techniques. *Adv Anal Chem Instrum* 1965; 117: 117–212.
15. Matsui Y, Tokunaga S. Internal reference compounds available for the determination of binding constants for cyclodextrin complexes by 1H NMR spectrometry. *Bull Chem Soc Jpn* 1996; 9: 2477–2480.
16. Johnson CS Jr. Diffusion ordered nuclear magnetic resonance spectroscopy: principles and applications. *Prog Nucl Magn Reson Spectrosc* 1999; 34: 203–256.
17. Schneider HJ *et al*. NMR studies of cyclodextrins and cyclodextrin complexes. *Chem Rev* 1998; 5: 1755–1786.
18. Berendsen HJC *et al*. Gromacs – a message-passing parallel molecular-dynamics implementation. *Comput Phys Commun* 1995; 1–3: 43–56.
19. Lindahl E *et al*. GROMACS 3.0: a package for molecular simulation and trajectory analysis. *J Mol Model* 2001; 8: 306–317.
20. Van der Spoel D *et al*. GROMACS: fast, flexible, and free. *J Comput Chem* 2005; 16: 1701–1718.
21. Hess B *et al*. GROMACS 4: algorithms for highly efficient, load-balanced, and scalable molecular simulation. *J Chem Theory Comput* 2008; 3: 435–447.
22. Oostenbrink C *et al*. A biomolecular force field based on the free enthalpy of hydration and solvation: the GROMOS force-field parameter sets 53A5 and 53A6. *J Comput Chem* 2004; 13: 1656–1676.
23. Darden T *et al*. Particle mesh Ewald: an N [center-dot] log(N) method for Ewald sums in large systems. *J Chem Phys* 1993; 12: 10089–10092.
24. Essmann U *et al*. A smooth particle mesh Ewald method. *J Chem Phys* 1995; 19: 8577–8593.
25. Berendsen HJC *et al*. Molecular dynamics with coupling to an external bath. *J Chem Phys* 1984; 8: 3684–3690.
26. Martínez JM, Martínez L. Packing optimization for automated generation of complex system's initial configurations for molecular dynamics and docking. *J Comput Chem* 2003; 7: 819–825.
27. Hermans J *et al*. A consistent empirical potential for water–protein interactions. *Biopolymers* 1984; 8: 1513–1518.
28. Mosmann T. Rapid colorimetric assay for cellular growth and survival: application to proliferation and cytotoxicity assays. *J Immunol Methods* 1983; 1–2: 55–63.
29. Szejtli J. *Cyclodextrin Technology*. Dordrecht: Kluwer Academic Publishers, 1998.
30. Terekhova I *et al*. Inclusion complex formation of $\alpha$- and $\beta$-cyclodextrins with riboflavin and alloxazine in aqueous solution: thermodynamic study. *J Incl Phenom Macrocycl Chem* 2011; 1: 167–172.
31. Zielenkiewicz W *et al*. Thermodynamic study on inclusion complex formation of riboflavin with hydroxypropyl-$\beta$-cyclodextrin in water. *J Therm Anal Calorim* 2010; 2: 595–600.
32. Loftsson T *et al*. Self-association and cyclodextrin solubilization of drugs. *J Pharm Sci* 2002; 11: 2307–2316.
33. Bekers O *et al*. Cyclodextrins in the pharmaceutical field. *Drug Dev Ind Pharm* 1991; 17: 1503–1549.
34. Wang XM, Chen HY. A spectroelectrochemical study of the interaction of riboflavin with beta-cyclodextrin. *Spectrochim Acta A Mol Biomol Spectrosc* 1996; 51: 599–605.
35. de Jesus MB *et al*. Improvement of the oral praziquantel anthelmintic effect by cyclodextrin complexation. *J Drug Target* 2010; 1: 21–26.
36. Giordano F *et al*. Thermal analysis of cyclodextrins and their inclusion compounds. *Thermochim Acta* 2001; 2: 123–151.
37. Ramamurthy V, Eaton DF. Photochemistry and photophysics within cyclodextrin cavities. *Acc Chem Res* 1988; 8: 300–306.
38. de Jesus MB *et al*. Theoretical and experimental study of a praziquantel and beta-cyclodextrin inclusion complex using molecular mechanic calculations and H1-nuclear magnetic resonance. *J Pharm Biomed Anal* 2006; 4: 1428–1432.
39. Cabeca LF *et al*. Topology of a ternary complex (proparacaine-beta-cyclodextrin-liposome) by STD NMR. *Magn Reson Chem* 2008; 9: 832–837.
40. de Araujo DR *et al*. Development and pharmacological evaluation of ropivacaine-2-hydroxypropyl-beta-cyclodextrin inclusion complex. *Eur J Pharm Sci* 2008; 1: 60–71.
41. Grillo R *et al*. Study of the interaction between hydroxymethylnitrofurazone and 2-hydroxypropyl-beta-cyclodextrin. *J Pharm Biomed Anal* 2008; 2: 295–302.
42. Edwards AM *et al*. Photochemical and pharmacokinetic properties of selected flavins. *J Photochem Photobiol B* 1999; 1: 36–41.

43. Williamson G *et al*. 1H NMR spectral analysis of the ribityl side chain of riboflavin and its ring-substituted analogs. *Methods Enzymol* 1986; 122: 240–248.
44. Chienthavorn O *et al*. Superheated water chromatography-nuclear magnetic resonance spectroscopy and mass spectrometry of vitamins. *J Pharm Biomed Anal* 2004; 3: 477–482.
45. Pinto LM *et al*. Physico-chemical characterization of benzocaine-beta-cyclodextrin inclusion complexes. *J Pharm Biomed Anal* 2005; 5: 956–963.
46. Moraes CM *et al*. Study of the interaction between S(-) bupivacaine and 2-hydroxypropyl-beta-cyclodextrin. *Int J Pharm* 2007; 1: 99–106.
47. Macomber RS. *A Complete Introduction to Modern NMR Spectroscopy*. New York: John Wiley & Sons, 1998.
48. Fraceto LF *et al*. Characterization of the inclusion complex ropivacaine: beta-cyclodextrin. *Quim Nova* 2007; 5: 1203–1207.
49. Morris KF, Johnson CS. Diffusion-ordered two-dimensional nuclear magnetic resonance spectroscopy. *J Am Chem Soc* 1992; 8: 3139–3141.
50. Bareford LM *et al*. Intracellular processing of riboflavin in human breast cancer cells. *Mol Pharm* 2008; 5: 839–848.
51. Loftsson T, Brewster ME. Pharmaceutical applications of cyclodextrins: effects on drug permeation through biological membranes. *J Pharm Pharmacol* 2011; 63: 1119–1135.

## Supporting Information

Additional supporting information may be found in the online version of this article.

**Movie S1** Representative movie from the molecular simulations of $\beta$-cyclodextrin and riboflavin from 5 to 15 ns. We represented the *x* and y periodic boundary condition molecules in transparent yellow. The z pbc molecules are not represented because they obscure the overall visualization. The hydrogen bonds are represented in orange.

**Movie S2** Representative movie from the molecular simulations of $\beta$-cyclodextrin and riboflavin from 35 to 45 ns. We represented the *x* and y periodic boundary condition molecules in transparent yellow. The z pbc molecules are not represented because they obscure the overall visualization. The hydrogen bonds are represented in orange.

Please note: Wiley-Blackwell are not responsible for the content or functionality of any supporting materials supplied by the authors. Any queries (other than missing material) should be directed to the corresponding author for the article.




 